Special Issue Papers

Laser Trapping in Cell Biology

WILLIAM H. WRIGHT, G. J. SONEK, Y. TADIR, AND MICHAEL W. BERNS

Abstract—**Optical traps offer the promise of being used as noninvasive micromanipulators for biological objects. We have developed an analytical model that accurately describes the forces exerted on dielectric microspheres while in a single-beam gradient force optical trap. The model can be extended to the trapping of biological objects. The model predicts the existence of a stable trapping point and an effective trapping range. A minimum trapping power of ~5 mW and an effective trapping range of 2.4 μm have been measured for 10 μm diameter dielectric microspheres, and are in reasonable agreement with expected results. In cell biology, we have used the optical trap to alter the movement of chromosomes within mitotic cells *in vitro* and to hold motile sperm cells. Results for the mitotic cells indicate that chromosome movement was initiated in the direction opposite to that of the applied force. Chromosome velocities as high as 48 μm/min were observed, and are 24 times faster than normal during cell division. In sperm trapping experiments, mean sperm velocities were unchanged following short (<30 s) exposures in the trap, while longer exposures resulted in a decrease in mean sperm velocities. Given its noninvasive nature, optical traps should prove to be useful tools in the study of biological processes.**

I. Introduction

It is now possible to use light, in the form of an optical trap, to manipulate microscopic objects without physical contact. In biology, an optical trap provides a new and novel tool for the manipulation of microorganisms and cells. Ashkin, *et al.*, first described the optical trapping of micrometer sized dielectric particles using the radiation pressure from two opposing laser beams [1]. While the single beam gradient force trap for atoms was also proposed [2], it was not until recently that this technique was applied to the optical trapping of microspheres [3]. Ashkin and co-workers were also the first to propose and demonstrate the use of optical traps for biological applications [4]–[6]. Various biological objects, including viruses, bacteria, yeast cells, and red blood cells have been trapped successfully, using both argon and Nd:YAG lasers in the single-beam configuration. From these studies, infrared laser traps were found to have a less detrimental effect on cell viability, compared to visible laser beams. Cell absorption is lower in the infrared. The use of radiation pressure and optical traps have subsequently been extended to cell manipulation and cell sorting [7], [8], and, very recently, to the measurement of the compliance of bacterial flagella [9].

Most of the aforementioned studies have been qualitative in nature. In order to effectively design optical traps for specific biological applications and, at the same time, predict the associated trapping forces, a quantitative understanding of the force generation process within an optical trap is required. We have, therefore, developed a model to describe the single-beam gradient force optical trap as it acts upon dielectric microspheres, and have compared our model to experimental results. Preliminary results from several biological systems are also reported.

For the work described herein, an optical trap was assembled by directing a 1.06 μm Nd:YAG laser beam into a conventional microscope and focusing the beam with a microscope objective. A model, based on geometrical optics, is presented to explain the behavior of a microsphere while caught in the optical trap. Polystyrene microspheres, having a diameter of 10 μm, were used as a model for biological cells [10], because of their similarity, both physically and optically, to tissue culture (e.g., Chinese hamster ovary) cells in suspension. To test the model, two experiments were performed. One experiment measured the minimum power required to trap the microsphere, while a second experiment determined the range over which a microsphere, initially caught in the trap, could be recovered. Results from both experiments corroborate the model presented herein.

In addition, we have conducted several experiments to demonstrate the use of optical traps in the study of biological systems. One set of experiments evaluated the effect of the single-beam optical trap on the velocity of motile spermatozoa [11]. Another set of experiments employed the optical trap to study chromosome movement during the process of cell division [12]. We note that the calculation of trap forces exerted on spermatozoa or chromosomes would require a more sophisticated model than presented here, and should take into account the structural properties, such as shape, and inhomogeneities of the cell itself.

Manuscript received July 7, 1989; revised November 10, 1989. This work was supported in part by the National Institutes of Health under Grant RR01192 and by the Strategic Defense Initiative Organization under Grant 84-88-C-0025.

W. H. Wright is with the Department of Electrical and Computer Engineering and the Beckman Laser Institute and Medical Clinic, University of California, Irvine, CA 92717.

G. J. Sonek is with the Department of Electrical and Computer Engineering, University of California, Irvine, CA 92717.

Y. Tadir and M. W. Berns are with the Beckman Laser Institute and Medical Clinic, University of California, Irvine, CA 92717.

IEEE Log Number 9040299.

A description of the dielectric microsphere model is presented in Section II of this paper. Experimental techniques and results of the microsphere experiments are presented in Sections III and IV, respectively. The results of experiments on chromosome and sperm trapping are described in Section V, along with a discussion of the cell fusion studies that are presently in progress. A summary of our work is given in Section VI.

II. The Dielectric Microsphere Model

The effects of a single-beam gradient optical trap on a biological object can be conveniently analyzed by considering the use of microspheres as a model system. Because dielectric microspheres are similar in size, shape, and refractive index to many different types of cells in suspension, they provide a good system for the analytical and experimental study of optical trap behavior. Limitations of the present model are described in a later section.

For spheres having dimensions that are much larger than the wavelength of light, the forces due to the radiation pressure of a focused laser beam can be calculated using a geometrical optics approach. To construct the model, we begin with a description of the forces associated with the reflected and transmitted light rays acting at a dielectric interface. The direction of the forces are found by tracing both skew and meridional rays of the laser beam through the sphere, both on, and off, the beam axis, in three dimensions. Finally, the power flowing through an infinitesimal area on the spherical surface, defined by each ray, is determined by integrating the beam intensity over that area. The total axial and transverse forces are then obtained by summing the force contributions from each ray over the surface of the sphere. The model assumes that there is negligible absorption of the light by the microsphere, and that the mechanism for momentum transfer to the microsphere, based upon totally elastic photon scattering at a dielectric interface, is the same for both the reflected and transmitted beams. In addition, only laser beams with Gaussian intensity profiles are considered.

In Fig. 1, we show the direction of the forces acting at each dielectric interface due to the reflected and transmitted beams. The forces are calculated at the points where the incident rays strike the sphere and where the transmitted rays leave the sphere. The magnitude of the forces due to reflection (F_r) and refraction (F_d) are

$$F_r = (2n_1PR/c)\cos(\alpha_1) \tag{1a}$$

$$F_d = (PT/c)\left(n_1^2 + n_2^2 - 2n_1n_2\cos(\alpha_1 - \alpha_2)\right)^{1/2} \tag{1b}$$

where R and T are the reflectance and transmittance of the beam at the dielectric boundary, n_1 and n_2 are the refractive indexes of the surrounding medium and the dielectric microsphere, respectively, α_1 and α_2 are the incident and transmitted angles, P is the total power incident on a small area of the sphere, and c is the velocity of light in free space. The term $2n_1P/c$ is recognized as the force exerted by a wave incident normal to a totally reflecting mirror immersed in a medium of index n_1.

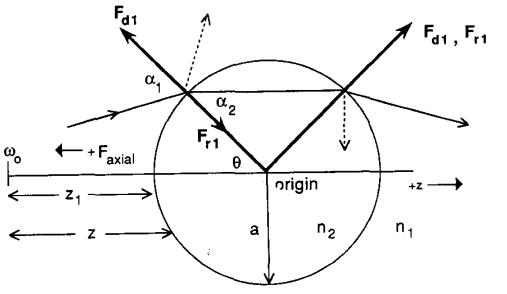

Fig. 1. Force components at a spherical surface. The thin solid ray is the incident beam, and continues through the sphere as the transmitted beam. The dashed rays correspond to the reflected beam at the two interfaces.

The radius of curvature of the Gaussian beam wavefront, given by

$$R(z) = z\left(1 + \left(\frac{\pi\omega_0^2}{\lambda z}\right)^2\right) \tag{2}$$

is used to determine the direction of the rays incident on the sphere. Here, ω_0 is the spot size of the focused laser beam in medium n_1, λ is the wavelength of light in medium n_1, a is the sphere radius, and $z = z_1 + a - a\cos\theta$ is the distance from the beam waist to the surface of the sphere. We define z_1 as the axial distance from the beam waist to the vertex of the sphere. Since $R(z)$ is always greater than the distance z, the rays appear to come from source points behind the beam waist. These rays are normal to the approximately spherical Gaussian wavefronts. Rays are traced through the microsphere in three dimensions using a skew-ray tracing procedure, as described by Born [13].

The power P in a Gaussian beam flowing through a small region of the spherical surface is calculated, in spherical coordinates, using the expressions

$$dS = a^2\sin(\theta)\,d\theta\,d\phi \tag{3}$$

$$r^2 = a^2\sin^2(\theta) + d^2 - 2ad\sin(\theta)\cos(\phi) \tag{4}$$

$$\omega^2(\theta) = \omega_0^2\left[1 + \left(\frac{\lambda(a - a\cos(\theta) + z_1)}{\pi\omega_0^2}\right)^2\right] \tag{5}$$

$$P = cn_1\epsilon_0E_1^2\omega_0^2\int\int\frac{1}{\omega^2(\theta)}\exp\left(\frac{-2r^2}{\omega^2(\theta)}\right)dS \tag{6}$$

where dS is a differential surface area on the microsphere and θ and ϕ are the polar and azimuthal angles in spherical coordinates, respectively.

Both the reflectance and transmittance at the dielectric boundary are a function of the polarization of the laser beam. We have assumed that the incident laser beam is linearly polarized, and calculate R and T for any angle ϕ as a combination of waves polarized parallel and perpendicular to the plane of incidence.

The results, obtained by numerically integrating (6), are shown in Fig. 2(a)–(d), where we depict the axial forces acting on the microsphere in a single-beam gradient optical trap, as a function of the distance z_1. The axial force

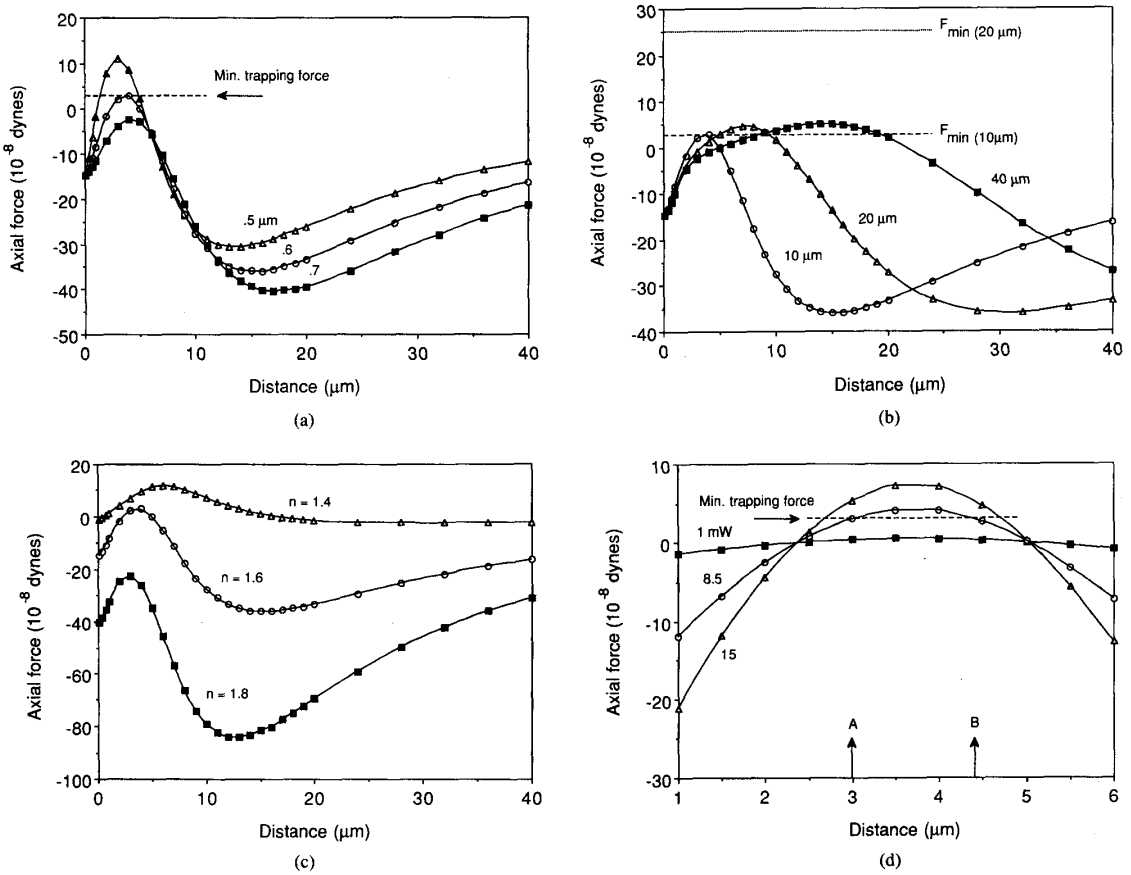

Fig. 2. (a) Calculation of the axial force on a microsphere for three different laser beam spot sizes as a function of the distance z_1. The sphere diameter is 10 μm ($n_2 = 1.6$), suspended in water ($n_1 = 1.33$). The incident laser power is 6 mW. (b) Calculation of the axial force on a microsphere for three different sphere diameters as a function of the distance z_1. The laser spot size is 0.6 μm. The incident laser power is 6 mW. The dotted line denoted by $F_{\min 10\mu m}$ and $F_{\min 20\mu m}$ indicate the minimum trapping force for the 10 and 20 μm spheres, respectively. (c) Calculation of the axial force on a 10 μm diameter microsphere for three different sphere refractive indexes as a function of the distance z_1. The laser spot size is 0.6 μm. Laser beam power is 6 mW. (d) Axial force on a 10 μm diameter microsphere ($n_2 = 1.6$) for three different laser power levels as a function of the distance z_1. The distance between A and B is defined as the effective trapping range. The spot size is 0.6 μm.

corresponds to the projection of F_d and F_r along the beam axis. We have defined the positive axial trapping force to be in the $-z$ direction. The laser beam propagates in the $+z$ direction, down through the microscope (Fig. 1). Parameters that were varied include beam spot size, sphere diameter, and the refractive index of the sphere. For all calculations, it was assumed that the dielectric microsphere was suspended in water ($n_1 = 1.33$).

Fig. 2(a) shows the axial force on a 10 μm diameter sphere, as a function of the distance z_1, for laser beam spot sizes of 0.5, 0.6, and 0.7 μm, respectively. The minimum trapping force, indicated by the dashed line in Fig. 2(a), corresponds to that force required to overcome the other forces acting on the microsphere. The net force acting on the 10 μm diameter polystyrene microsphere in the axial (vertical) direction, when radiation pressure is not present, is simply equal to the difference between the gravitational and buoyant forces ($\boldsymbol{F}_g - \boldsymbol{F}_b$) and is approximately $3 \cdot 10^{-8}$ dyn. We note that the trap is more effective at confining the sphere as the spot size is decreased, due to the fact that there is an increase in the axial force directed towards the beam waist. When the spot size is 0.7 μm, for example, an optical trap is not created at all. Instead, the sphere is always pushed in the direction of the beam away from the beam focus.

In Fig. 2(b), we show the axial force on a sphere for sphere diameters of 10, 20, and 40 μm, as a function of the distance z_1. The laser spot size was chosen to be 0.6 μm. For an incident beam power of 6 mW, only the 10 μm diameter spheres are trapped. This occurs because both the 20 and 40 μm diameter spheres have minimum trapping force requirements that are greater than the net

axial force produced by the optical trap. The minimum force for the latter is not shown on this graph, since it has a value of $\sim 2 \cdot 10^{-6}$ dyn. We can see that the peak of the force curve shifts to greater distances away from the beam waist as the sphere diameter increases.

Fig. 2(c) examines the effect of the microsphere refractive index on the axial force, as a function of the distance z_1, for a spot size of 0.6 μm. Trapping forces are obtained only for the $n = 1.4$ and $n = 1.6$ refractive index 10 μm diameter spheres. In the limiting case, when the refractive index of the surrounding medium n_1 is equal to the refractive index of the sphere n_2, there is no force acting on the sphere. Alternatively, when n_1 is greater than n_2, the sphere is always pushed out of the laser beam, as in the case of air bubbles trapped in glycerol [1].

Finally, in Fig. 2(d), we show the dependence of the axial force on the incident laser power. From (1a) and (1b), we expect the axial force to scale linearly with power. This behavior is reflected in the curves of Fig. 2(d), from which we can predict the behavior of the microsphere within the optical trap. Again, the minimum force required for trapping is indicated by the dashed line. A stable trap is defined as the point where the net force on the microsphere is equal to zero and where restoring forces act to keep the microsphere at the equilibrium point. This occurs at point A, where the trap generated force equals the difference between the gravitational (F_g) and buoyant (F_b) forces acting on the microsphere. When the microsphere is at a distance $z_1 < A$ from the beam waist, it is pulled towards the trap by gravity and may also be pushed by the optical beam. For a microsphere located a distance $A < z_1 < B$, it is pulled back into the trap by the optical beam. Finally, if the microsphere lies at a distance $z_1 > B$, it remains untrapped. The region $z_1 < B$ defines the range over which the trap is functional in confining the microsphere, while the region $A < z_1 < B$ defines an effective trapping range, i.e., the distance over which the axial force exceeds the minimum trapping force. We note that, for very large distances from the beam waist, the axial force on the microsphere approaches zero.

Our model also provides information about the transverse (i.e., radial) forces exerted on a microsphere in the optical trap. Fig. 3 depicts the transverse force on a microsphere as a function of the distance the sphere is offset laterally from the laser beam axis. Two curves are presented, showing the variation in force for a beam waist located 5 or 10 μm from the vertex of the microsphere. As expected, the force is zero when the sphere is centered on the beam axis. The force reaches a maximum at an offset distance approximately equal to the sphere radius and then approaches zero for large offset distances. The transverse force is a restoring force that acts to pull the microsphere back to the center of the trap. The curves presented in Fig. 3 are similar in form to those presented in [14] for a homogeneous microsphere in a Gaussian laser beam.

From Fig. 2(a), it can be seen that in order to effectively trap the 10 μm dielectric microspheres used in this study, the optical trap should have a maximum spot size of <0.7 μm. Below the maximum spot size, there are

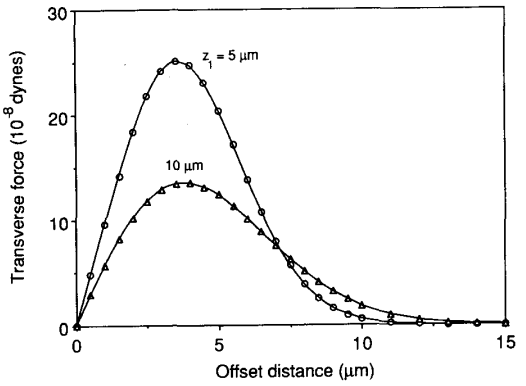

Fig. 3. Calculation of the transverse force on a microsphere as a function of the offset distance transverse to the beam axis. Two curves are presented, showing the variation in the force with the distance z_1. The sphere diameter is 10 μm ($n_2 = 1.6$), spot size is 0.6 μm, and the beam power is 1 mW.

many possible combinations of ω_0 and power P that will result in a trapped microsphere. Experimental confirmation of these results are presented in Section IV.

III. Single-Beam Optical Trapping System

The system used in our experiments for optical trapping is depicted in Fig. 4. A continuous wave Nd:YAG laser (Quantronix Model 116), operating at a wavelength of 1.06 μm in the fundamental TEM_{00} mode, was first passed through a 570 nm low-pass filter. The filter was used to block the 532 nm signal that was generated by a frequency doubling crystal within the laser cavity. The beam was then passed through a variable attenuator (Newport Model 930-5), followed by a Glan–Thompson polarizing prism. In order to monitor the laser power at the entrance to the trap, a quartz coverslip was used to reflect a portion of the vertically polarized beam into a silicon photodiode. A neutral density filter ($ND = 4.0$) was placed in front of the detector to prevent overloading.

The photodiode output was calibrated with respect to the laser power transmitted through the input optical system, consisting of the objective lens, immersion oil, and a coverslip. Subsequent to establishing a power calibration curve prior to each experiment, the laser beam was directed into a microscope (Zeiss Photomicroscope III), using a dichroic mirror that reflected the laser wavelength and transmitted shorter wavelengths. A 100× objective lens (Zeiss Neofluar, numerical aperature = 1.3) was used to focus the laser beam and create the optical trap. Immersion oil ($n = 1.52$) was placed between the lens and the coverslip to index match the high power objective. A 15 cm positive lens, located above the microscope, was used to focus the laser beam into the microscope system.

The microscope image was projected onto a video camera located above the microscope. An infrared (IR) absorbing filter was placed in front of the camera lens to block the IR laser beam reflected back from optical elements in the beam path. The video signal from the camera

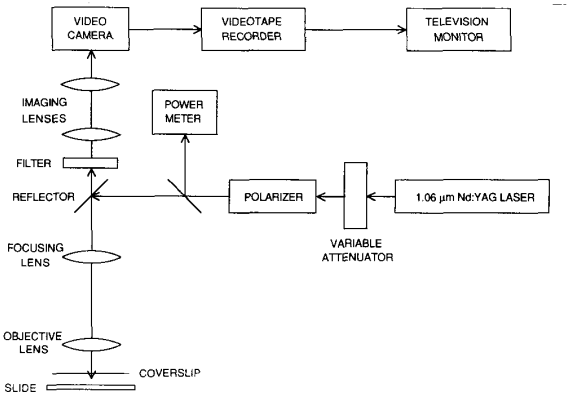

Fig. 4. Schematic of the optical trapping system.

was sent either to a video tape recorder or to the input of an image array processor. The recorded images were subsequently analyzed using an image processing system [15], that produced a 512 × 512 pixel image with a gray scale of 256 (8 b) and a video rate of 30 frames/s. This method was used to measure the spot size of the focused laser beam produced by the objective lens.

For the trapping experiments involving microspheres, a special chamber was built, consisting of a 3 × 5 cm sheet of parafilm, having a thickness of ≈ 130 μm and a hole in its center, sandwiched between two 0.17 mm thick coverslips. Commercial microspheres, made of polystyrene material having a density, relative to water, of 1.06 and a refractive index $n = 1.6$ [16] were suspended in water ($n = 1.33$), and then placed in the well created by the parafilm, before being sealed with the coverslips. Finally, the coverslips were sandwiched between two aluminum plates to form a sealed chamber. An aperture on each side of the plates allowed the simultaneous imaging and trapping of the microspheres within the chamber.

IV. Optical Trapping of Polystyrene Microspheres

A. Experimental Results

Knowledge of the minimum trapping power and effective trapping range are critical to understanding the effects of an optical trap on a biological medium. As a first step, these parameters were quantified for uniform polystyrene microspheres in the single-beam optical trapping system. Two experiments were therefore designed and performed to test the dielectric microsphere model, as presented in Section II. The first experiment determined the minimum laser power required to hold polystyrene microspheres in a single-beam optical trap. The second experiment determined the maximum period of time that it takes for a microsphere to be released from the trap, and subsequently be recaptured. This provides an indirect measurement of the distance between points A and B in Fig. 2(d), defined as the effective trapping range. Both experiments rely upon the ability to achieve a balance between the axial force exerted by the laser beam on the sphere, and the difference between the gravitational ($\boldsymbol{F}_g$) and buoyant forces ($\boldsymbol{F}_b$) exerted on the sphere.

The minimum power required to hold the microsphere in the trap was measured for a 100× objective. We note that, as indicated in Fig. 2(a), lower power objectives, which have larger beam waists, would not be expected to provide an axial force component that is directed towards the beam waist. Using the 100× objective, a microsphere adhering to the upper coverslip was pushed away from the coverslip and into the trap using a laser power of ~25–50 mW, a power much larger than the minimum power required for trapping. The microsphere was then moved just below the coverslip by focusing the microscope. The trapping force was then decreased by attenuating the laser beam. Once the sphere fell out of the trap, the power measured at the beamsplitter location, as indicated in Fig. 4, was recorded. The power at the sphere was then determined using a calibration curve established prior to the actual experiment. The results of the power threshold experiments, as described above, are summarized in Table I.

A second experiment was designed to measure the effective trapping range, or the axial distance over which a sphere could be caught and held within the trap. The distance was measured by observing the maximum time the trap could remain off before the sphere fell outside of the trap range. By assuming that the microsphere moves at a terminal velocity during the interval of time that the trap is off, the total distance d traveled by the moving microsphere is given by $V_t t$, where V_t is the terminal velocity. A 10 μm microsphere, moving in water, achieves a terminal velocity of ~3.2 μm/s within ~7 μs, in the absence of trapping forces. In comparison, the average time it takes for the microsphere to move a distance that is beyond the reach of the optical trap is on the order of seconds. The viscosity of the water was taken to be 0.01 dyn · sec/cm^2 at 20°C [17]. The results of the effective trap range measurements are summarized in Table II.

B. Discussion

The results presented in Tables I and II are in good agreement with the calculated values presented in Fig. 2(a) and (d). The discrepancies can, for the most part, be attributed to the uncertainties associated with the measurement of key parameters, such as the focused spot size, the precise location of the beam waist, and the laser beam power at the objective.

The measurement of the minimum laser power required to hold a microsphere against the force $\boldsymbol{F}_g - \boldsymbol{F}_b$, when used in conjunction with the results of Fig. 2(a) and (d), provides an indirect determination of the axial force generated by the optical trap. From Table I, this threshold power was found to be between 4 and 9 mW, respectively. Knowing that the force required to hold the microsphere, $\boldsymbol{F}_g - \boldsymbol{F}_b$, is $\sim 3 \cdot 10^{-8}$ dyn, we can use the model to predict the power needed to hold the microsphere. From both figures, the threshold power is approximately 6 mW for a spot size of 0.6 μm. It can be seen

TABLE I
RESULTS OF THE AXIAL FORCE MEASUREMENTS. THE NUMBER OF MICROSPHERES IN EACH EXPERIMENT IS INDICATED BY n. THE ERROR INDICATED IS THE STANDARD DEVIATION OF THE MEASURED POWER. THE POWER MEASUREMENT HAD AN ACCURACY OF $\pm 5\%$. THE MODEL PREDICTS A THRESHOLD POWER OF ~ 6 mW FOR A SPOT SIZE OF 0.6 μm

Exp. No.	n	Power (mW)
1	20	9.1 ± 1.91
2	20	5.8 ± 1.26
3	20	4.6 ± 0.84
4	20	4.1 ± 0.73
5	20	7.5 ± 0.94

TABLE II
RESULTS OF THE EFFECTIVE TRAPPING RANGE MEASUREMENTS. THE INDICATED ERROR IS THE STANDARD DEVIATION OF THE MEASURED POWER AND TIME, RESPECTIVELY. THE ACCURACIES WERE $\pm 5\%$ FOR THE POWER MEASUREMENTS AND ± 0.1 S FOR THE TIME MEASUREMENTS. THE MODEL PREDICTS AN EFFECTIVE TRAPPING RANGE OF ~ 1.4 μm FOR A SPOT SIZE OF 0.6 μm

Exp. No.	n	Power (mW)	Time (s)	Distance (μm)
1	10	24.2 ± 0.25	2.34 ± 0.41	7.6
2	14	8.5 ± 0.26	0.73 ± 0.26	2.36
3	20	8.6 ± 0.38	0.75 ± 0.15	2.43

that the values are in good agreement with each other. However, we note that the axial force measurements are very much dependent upon, and sensitive to, the spot size of the laser beam. Likewise, the distance between points *A* and *B* in Fig. 2(d), defined earlier as the effective trapping range, was calculated to be approximately 1.4 μm for a spot size of 0.6 μm and an incident laser power of ~ 8.5 mW. This distance was measured to be ~ 2.4 μm, as shown in Table II. The error associated with the measurement of the laser beam power was estimated to be $\sim \pm 5\%$, while the power stability of the laser output was estimated to be $\pm 10\%$. This latter effect was the likely cause of microsphere jitter for particles caught in the trap.

While the measurements described above nicely validate the microsphere model, it should be noted that the measurements only provide information on the magnitude of the peak axial force and the effective trapping range. The measurements do not provide values for the forces over a large portion of distances away from the beam waist location, nor do they indicate the absolute locations of the crossing points *A* and *B* with respect to the location of the laser beam waist. Because diffraction effects have been ignored, it is expected that greater accuracy can be achieved if a light scattering approach is taken. The size parameter, or the ratio of the sphere circumference to the wavelength, is 39 and the relative refractive index is 1.2 for our system. We obtained, to within a factor of two, correlation between the model and experimental results. Therefore, the geometrical optics approximation appears to provide a good description of the trapping process.

The greatest uncertainty in the experimental measurements described above results from the measurement of the spot size of the focused laser beam that forms the optical trap. From Fig. 2(a), it is evident that the focal spot size of the laser beam is a key parameter in determining the axial force on the microsphere. For the spot size measurements, the mirrored surface of a neutral density (ND = 2.0) filter was used to reflect the focused laser beam back through the optical system and into the video camera. The spot size was determined by counting the number of pixels, vertically or horizontally, from a video image and multiplying this number by a calibration factor that was determined using a stage micrometer. A measurement of the spot size at the beam waist, for the 15 cm focusing lens and the 100× objective, with immersion oil, indicated that the spot diameter was ~ 1.2–1.6 μm $\pm$ 0.1 μm. This range in spot size was due to the ellipticity of the observed beam. To compare the model with our experimental results, we used a spot size of 0.6 μm, which corresponds to the expected size of a diffraction limited spot formed by the 100× objective at 1.06 μm. Owing to the complex optical system of the microscope, attempts to correlate measured and calculated spot size values were unsuccessful. It is likely that another method of measuring the spot size is needed to verify the results obtained using the video system technique. We note, however, that our spot size measurement technique is similar, in principle, to spot size measurements made with photographic film. Other methods may provide better results [18]. In addition, it was found that, experimentally, a change in the focal length of the microscope focusing lens has a dramatic effect on the performance of the trap. For example, the trap functioned properly for the short focal length lenses of 10 and 15 cm, but was unable to trap particles when lenses of longer focal length were used. As indicated in Fig. 2(a), this also results in a change in the spot size at the trap.

In the present system, the requirement that both imaging and laser beam manipulation be performed by the same focusing lens creates another serious design constraint. It was not possible, for example, to have the beam waist located in the same plane as the object plane and simultaneously meet the requirement for both minimum spot size, and imaging of the object plane at infinity. The beam waist was measured to be 5.5 $\pm$ 0.5 μm below the object plane of the microscope. We compare this to a calculated value of ~ 10 μm, based upon a Gaussian beam transformation calculation for a beam passing through the microscope. Our goal was, therefore, to obtain the smallest spot size without the introduction of significant distortion to the beam intensity profile. Shorter focal length lenses generally produced some degree of beam profile distortion, as observed in the far field, while longer focal length lenses, which minimized diffraction effects, often led to larger spot sizes and a less effective trap. Clearly, for op-

timal trapping, a tradeoff exists between spot size and laser beam profile, as predicted by Dickson [19]. At present, the microsphere model, as previously described, does not consider non-Gaussian beam profiles. In comparison to our system, the single-beam gradient trap of Ashkin [5], [6] separated the manipulation of the trapping beam from the imaging of the specimen. Therefore, many of the problems described above were not encountered.

V. Application to Cell Biology

Our goal in developing the microsphere model was to explain the performance of the optical trap acting on biological objects in terms of the forces generated by the trap. The two biological studies presented herein are significant since they employ the optical trap as a force generator. The experiments involving chromosome movement in mitotic cells may prove to be of use in resolving long-standing questions regarding the mechanisms of chromosome movement in cells, if the trap can be calibrated in terms of the force it exerts on the chromosome. Another important application of the optical trapping technique is in the micromanipulation of spermatozoa. The noninvasive feature of the optical trap may prove to be less damaging to sperm during the manipulation process, compared to conventional techniques. Quantitative measurements of force generation by motile cells may also be advanced with the help of a calibrated optical trap.

A. Studies of Chromosome Movement in Mitotic Cells

For the chromosomal studies performed, Potorous tridactylis (PTK_2) rat kangaroo kidney cells were grown in culture on 0.17 mm thick glass coverslips and maintained at a temperature of 35–37°C. This cell type was selected because the chromosomes are clearly visible during the process of cell division [20]. A 10 cm lens was used to focus the laser beam into the microscope instead of the 15 cm lens described earlier. The resulting trap for the shorter focal length lens was just as effective as before, even though the beam profile exhibited slightly more distortion.

The optical trap was used to exert a transverse force on chromosomes in two cases; first, for centrophilic chromosomes located off the mitotic spindle between one pole and the edge of the cell, and then, for late moving chromosomes located between the metaphase plate and one mitotic pole. Control experiments were performed by applying the trap to other regions of the cell, with no effect on mitosis. The results of the chromosome trapping experiments are depicted in Fig. 5. Digital image processing was used to improve the quality of the images stored on the videotape [15].

For the stationary centrophilic chromosome not yet on the metaphase plate, the chromosome, shown in Fig. 5(a), reoriented and moved towards the spindle pole, a distance of 11 μm away, as seen in Fig. 5(b), and arrived at the spindle pole 45 s later as shown in Fig. 5(c). The measured peak velocity of ~ 48 μm/min was 24 times higher than the nominal values reported for this cell type [20]. A graph of the chromosome velocity over time, after application of the laser trap, is shown in Fig. 6. After the chromosome reached the pole and stopped, the trap was moved to the side of the chromosome facing the pole, shown in Fig. 5(c), and then was reapplied. Once again, the chromosome moved away from the trap in a transverse direction, as seen in Fig. 5(d), this time towards the metaphase plate at a maximum velocity of ~ 4.4 μm/min. Fig. 5(e) shows the chromosome at the metaphase plate. A second experiment involving late moving chromosomes, using a trap power of ~ 40–50 mW, initiated movement of stationary chromosomes towards the metaphase plate. Maximum velocities of 20 μm/min and 18 μm/min were observed for two chromosomes from two different cells, respectively. It is not known at this time what minimum power is required to initiate chromosome movement.

B. Trapping of Spermatozoa

Sperm trapping was performed using a 40× Neofluar objective (Zeiss), instead of the 100× objective used in the microsphere experiment, on specimens moving in a direction transverse to the focused laser beam. The 40× objective has a greater field of view and, as a result, facilitated measurement of the sperm velocity and also resulted in an increased spot size. The power of the trap was measured to be 1 W $\pm$ 100 mW at the objective. A high power level was used to ensure trapping of highly motile sperm. A motorized X–Y microscope stage was used to move the sperm confined in the optical trap. A 10 cm lens replaced the 15 cm lens used in the microsphere studies. The sperm velocity was measured before and after trapping, using the digital image processing system previously described. Experiments were performed on a glass slide under a 0.15 mm thick coverslip 4–8 h following ejaculation, using morphologically normal sperm. Exposure times for the sperm in the trap ranged from 15 to 120 s.

Results for the sperm trapping experiments are presented in Fig. 7. The mean sperm velocity did not change significantly for exposure times of 30 s or less in the optical trap. However, longer exposure times resulted in a gradual decrease in the mean linear velocity. A statistical t-test was used to gauge the significance of the difference between the mean velocities before and after exposure to the optical trap. The significance is expressed in terms of the p-value, which is the probability that the two mean values are not different, as shown in Fig. 7. The optical trap also affected the pattern of sperm motility. For example, of the initial sperm population, 39% were classified as straight progressing, and another 58% had a zigzag pattern as they swam through the medium. For exposure times of 30 s or less in the optical trap, there was little change in the motility pattern of initially straight progressing sperm. However, 40% of the sperm with an initial zigzag pattern changed to a straight progressing pattern upon release from the trap. Other measured parameters are discussed in more detail elsewhere [11].

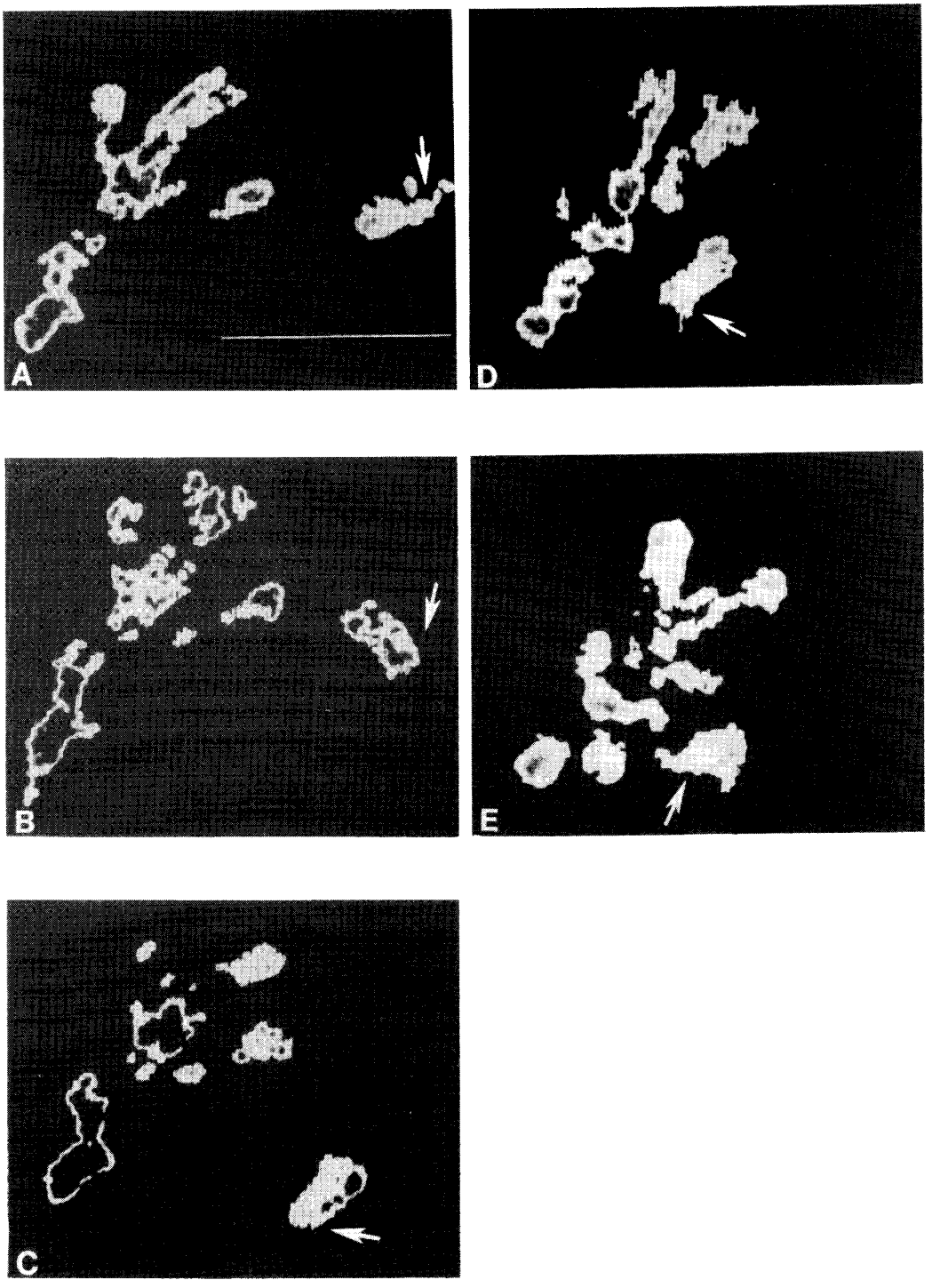

Fig. 5. (a) A cell with a single chromosome off the mitotic spindle. The optical trap was focused to a point adjacent to the chromosome, as indicated by the arrow. (b) The chromosome has changed orientation and is moving towards the lower spindle pole. (c) The chromosome is at the spindle pole. Subsequently, the optical trap was reapplied at the point indicated by the arrow. (d) Now the chromosome is moving towards the metaphase plate, located midway between the two spindle poles. (e) The chromosome is at the metaphase plate.

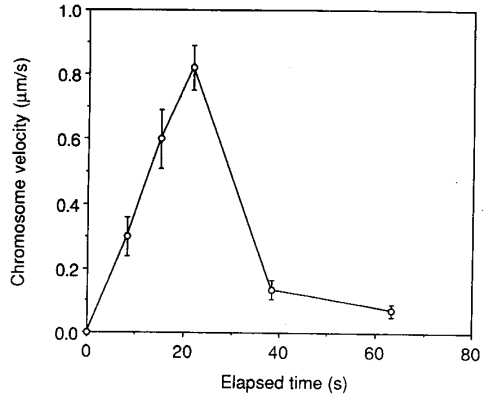

Fig. 6. Chromosome velocity versus time for the cell shown in Fig. 5.

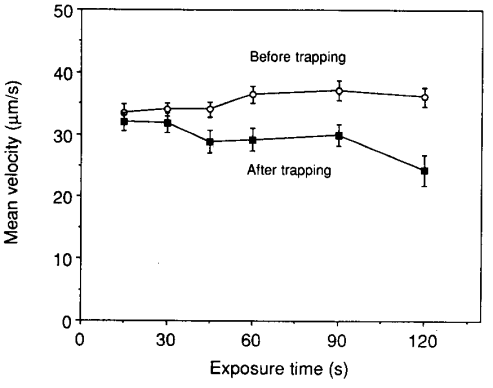

Fig. 7. Results of the sperm trapping experiments. Sperm velocity was measured before and after exposure to the optical trap and is expressed as the mean for each exposure class. The error bars indicate the standard error of the mean. A total of 514 sperm were evaluated, with 63 to 97 sperm in each exposure group. For exposure times of 30 s or less, the change in velocity was not significant. Changes in velocity as a result of exposure times of 45 s or longer were significant ($p < 0.012$ for $t = 45$ s; $p < 0.0001$ for $t > 45$ s).

C. Summary of Biological Experiments

As described above, the experiments employing mitotic cells have demonstrated that the forces exerted on chromosomes during cell division, by the chromosome movement motors, can be stimulated to function in response to an opposing force. In this case, the opposing force is a pulling force exerted by the optical trap in a transverse direction (Fig. 3). Furthermore, they demonstrate that chromosomes can be moved at velocities much higher than previously thought possible [12].

The ability to hold and manipulate sperm may be useful in clinical procedures, such as for fertilization *in-vitro*, as well as in the laboratory to evaluate the effect of drugs on sperm motility. A serious concern is the possible damage to the sperm, from absorption and subsequent heating, after exposure to the trap. We did not address this question directly in the sperm experiments other than to observe the altered motility patterns. Further studies involving electron microscopy, as well as functional assays to measure fertilization rates for optically trapped sperm, are necessary. We are currently studying the relationship between sperm velocity and the laser power required to hold the sperm. In conjunction with an extension of the theoretical model presented herein, it should be possible to calibrate the optical trap in terms of the transverse force it exerts on the sperm cells.

Other applications of the optical trap presently being pursued include the trapping of cells targeted for cell fusion. Current methods of cell fusion are handicapped by the lack of selectivity regarding the choice of cells that participate in the fusion process. The optical trap would allow a user to select the specific *B*-lymphocyte, that produces the desired antibody, to be joined with a myeloma cell into a hybridoma, as well as manipulating the hybridoma after the fusion process. Once the two cells are in the optical trap, a second laser, in this case a frequency tripled Nd:YAG laser operating at a wavelength of 355 nm, would be used to break down the membrane and induce the cell fusion. Some of the advantages of using the optical trap for cell fusion might include improved cell selectivity over current methods, increased efficiency in the production of desired hybridomas, and the ability to bring cells into close proximity during the fusion process. One of the problems presently encountered with this application is in the suitable design of the trapping chamber [21]. Related progress in cell manipulation and chamber design has previously been reported [7], [8].

An understanding and analysis of the aforementioned biological trapping experiments is hindered by the lack of available information regarding the optical and physical properties of the biological objects in the trap. Key optical properties that need to be determined include the refractive index and absorption of the cell or chromosome, respectively. Some of the physical properties of the cell that need to be characterized include the shape, composition, and surface charge. Other considerations might include the deformation dynamics of the cell while in the trap. Increased knowledge of the optical and physical properties should lead to improvements in the correlation of the model with experimental measurements.

VI. Conclusions

In summary, a model has been developed which quantifies, for the first time, the forces acting on dielectric microspheres in a single-beam gradient force optical trap. In comparison to previous studies, the present model is used to predict, while confined in the trap, the location of the microsphere and the existence of an effective trapping range resulting from a negatively directed axial trapping force. Experimental results are in good agreement with model predictions.

The focused spot size, and its location with respect to the object plane of the microscope, are found to be important design parameters for the single beam optical trap. These parameters are controlled by the microscope optics and the optical components external to the microscope. As a consequence, a tradeoff exists between the spot size of the focused laser beam and the forces generated in the

optical trap. Increasing the trapping force requires a smaller spot size, which, in turn, leads to distortion of the Gaussian laser beam profile.

Finally, we have demonstrated the application of an optical trap to several biological systems. Two experiments have been described which demonstrate the use of the optical trap as a tool for the study of fundamental problems in cell biology and sperm physiology. Furthermore, the optical trap may find application as a commercial device for cell manipulation.

ACKNOWLEDGMENT

The authors are indebted to L. Liaw for her expert assistance in the preparation of Fig. 5. Construction and operation of the optical trap was skillfully performed by J. Andrews and G. Profeta. We also thank O. Vafa, B. J. Tromberg, and R. Wiegand Steubing for helpful discussions, as well as H. Gamo for suggesting the use of dielectric microspheres as a model for biological cells.

REFERENCES

[1] A. Ashkin, "Acceleration and trapping of particles by radiation pressure," *Phys. Rev. Lett.*, vol. 24, pp. 156–159, 1970.
[2] ——, "Trapping of atoms by resonance radiation pressure," *Phys. Rev. Lett.*, vol. 40, pp. 729–732, 1978.
[3] A. Ashkin, J. M. Dziedzic, J. E. Bjorkholm, and S. Chu, "Observation of a single-beam gradient force optical trap for dielectric particles," *Opt. Lett.*, vol. 11, pp. 288–290, 1986.
[4] A. Ashkin, "Applications of laser radiation pressure," *Science*, vol. 210, pp. 1081–1088, 1980.
[5] A. Ashkin and J. M. Dziedzic, "Optical trapping and manipulation of viruses and bacteria," *Science*, vol. 235, pp. 1517–1520, 1987.
[6] A. Ashkin, J. M. Dziedzic, and T. M. Yamane, "Optical trapping and manipulation of single cells using infrared laser beams," *Nature*, vol. 330, pp. 769–771, 1987.
[7] T. N. Buican, M. J. Smith, H. A. Crissman, G. C. Salzman, C. C. Stewart, and J. C. Martin, "Automated single-cell manipulation and sorting by light trapping," *Appl. Opt.*, vol. 26, pp. 5311–5316, 1987.
[8] T. N. Buican, D. L. Neagley, W. C. Morrison, and B. D. Upham, "Optical trapping, cell manipulation, and robotics," *Proc. SPIE*, Symposium on Medical Applications of Lasers and Optics, Los Angeles, CA, 1989.
[9] S. M. Block, D. F. Blair, and H. C. Berg, "Compliance of bacterial flagella measured with optical tweezers," *Nature*, vol. 338, pp. 514–518, 1989.
[10] W. H. Wright, G. J. Sonek, and M. W. Berns, "Optical trapping of microspheres as a model for biological cells," presented at the 11th Int. Conf. IEEE Eng. Med. Biol. Soc., Seattle, WA, 1989.
[11] Y. Tadir, W. H. Wright, O. Vafa, T. Ord, R. H. Asch, and M. W. Berns, "Micromanipulation of sperm by a laser generated optical trap," *Fertility and Sterility*, vol. 52, pp. 870–873, 1989.
[12] M. W. Berns, W. H. Wright, B. J. Tromberg, G. A. Profeta, J. J. Andrews, and R. J. Walter, "Use of a laser-induced optical force trap to study chromosome movement on the mitotic spindle," *Proc. Nat. Acad. Sci. USA*, vol. 86, pp. 4539–4543, 1989.
[13] M. Born and E. Wolf, *Principles of Optics*, 2nd (revised) ed. New York: Macmillan, 1964, sec. 4.9.3.
[14] J. S. Kim and S. S. Lee, "Scattering of laser beams and the optical potential well for a homogeneous sphere," *J. Opt. Soc. Amer.*, vol. 73, pp. 303–312, 1983.
[15] R. J. Walter and M. W. Berns, "Computer-enhanced video microscopy; digitally processed microscope images can be produced in real time," *Proc. Nat. Acad. Sci. USA*, vol. 78, pp. 6927–6931, 1981.
[16] *CRC Handbook of Chemistry and Physics*, 60th ed. Boca Raton, FL: CRC, 1979, p. C-785.
[17] *CRC Handbook of Chemistry and Physics*, 60th ed. Boca Raton, FL: CRC, 1979, p. F-51.
[18] M. B. Schneider and W. W. Webb, "Measurement of submicron laser beam radii," *Appl. Opt.*, vol. 20, pp. 1382–1388, 1981.
[19] L. D. Dickson, "Characteristics of a propagating Gaussian beam," *Appl. Opt.*, vol. 9, pp. 1854–1861, 1970.
[20] P. A. McNeil and M. W. Berns, "Chromosome behavior after laser microirradiation of a single kinetochore in mitotic PtK2 cells," *J. Cell Biol.*, vol. 88, pp. 543–553, 1981.
[21] R. Wiegand Steubing, personal communication.

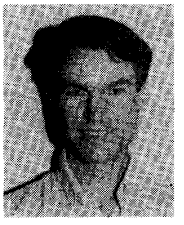

William H. Wright received B.S. degrees in electrical engineering and biological sciences and the M.S. degree in electrical engineering from the University of California, Irvine, in 1981, 1982, and 1989, respectively.

He is currently a graduate student with the Department of Electrical Engineering, University of California, Irvine, working towards the Ph.D. degree. He is also employed as an engineer and conducts his research at the Beckman Laser Institute and Medical Clinic. His research interests include optical traps, laser microsurgery and spectroscopy of cells, and laser–tissue interactions.

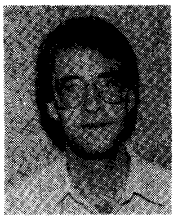

G. J. Sonek received the B.S. degree in physics from the Polytechnic Institute of New York, Brooklyn, and the M.S. and Ph.D. degrees in applied physics from Cornell University, Ithaca, NY, in 1979, 1982, and 1986, respectively.

Since 1986, he has been an Assistant Professor of Electrical and Computer Engineering with the University of California, Irvine. His research interests include the study of integrated optical, guided wave, and optoelectronic devices for lightwave communications, signal processing, and optical computing; and the study of laser interactions in biological media.

Dr. Sonek is a member of the American Physical Society, the IEEE Lasers and Electro-Optics Society, SPIE, Sigma Pi Sigma, Sigma Xi, and Eta Kappa Nu.

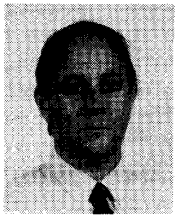

Y. Tadir is the Director of the In Vitro Fertilization and Laser Program of the Beilinson Medical Center at Tel Aviv University (Sakler School of Medicine). He was on sabbatical at the Institute during 1988–1989. While at the institute, he conducted research, using laser microbeams and photodynamic therapy, to develop methods that may be useful in the treatment of infertility.

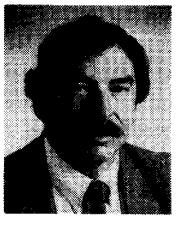

Michael W. Berns, received the B.S., M.S., and Ph.D. degrees from Cornell University, Ithaca, NY, specializing in genetics, cell biology, and development biology.

He is currently a Professor of Surgery and Cell Biology, Radiology, and Ophthalmology and organized the University of California, Irvine's laser research and treatment programs and is President and cofounder of the Beckman Laser Institute and Medical Clinic. He began using lasers to perform cell microsurgery in the early 1960's. His basic research interests have focused on studies on cell genetics, cellular motility and cell movement, and the development of lasers and computers for biomedical studies. His clinical research involves the use of the laser in cancer, cardiovascular surgery, and vision. He has published over 200 research articles and has authored and/or edited four books that have been translated into Chinese, Japanese, Italian, and Serbo-Croatian. He has served on advisory panels to the U.S. National Academy of Sciences, the National Institutes of Health, the American Institute of Biological Sciences, the European Physical Society, and the American Society for Lasers in Medicine and Surgery, as well as serving as President of the latter. He has held appointments as Visiting Professor at Moscow State University, Moscow, U.S.S.R. and the Genetics Institute, Academia Sinica (PRC). He has recently been named to fill the Arnold and Mabel Beckman Endowed Chair in Laser Biomedicine at the University of California.